ARTICLE
Journal of Cellular Biochemistry 114:162–173 (2013)

Journal of Cellular Biochemistry

HSPB1 is an Intracellular Antiviral Factor Against Hepatitis B Virus

Shi-Wen Tong, Yi-Xuan Yang, Huai-Dong Hu, Xuan An, Feng Ye, Hong Ren, Sang-Lin Li, and Da-Zhi Zhang*

Key Laboratory of Molecular Biology for Infectious Diseases of Ministry of Education of China, The Second Affiliated Hospital, Chongqing Medical University, Chongqing 400016, China

ABSTRACT

Hepatitis B virus (HBV) is the most common of the hepatitis viruses that cause chronic liver infections in humans and it is considered a major global health problem. However, the mechanisms of HBV replication are complex and not yet fully understood. In this study, the HBV DNA-transfected HepG2.2.15 cell line and its parental HepG2 cell line were analyzed by isobaric tags for relative and absolute quantitation (iTRAQ)-coupled two-dimensional liquid chromatography tandem mass-spectrophotometry (2D LC-MS/MS), a successfully exploited high-throughput proteomic technology. In total, 2,028 unique proteins were identified and 170 proteins were differentially expressed in HepG2.2.15 cells as compared with that in HepG2. Several differentially expressed proteins were further validated by Western blot and real-time quantitative reverse transcription-PCR. Furthermore, the association of HBV replication with heat shock protein B1, one of the highly expressed proteins in HepG2.2.15 cells, was verified. HSPB1 functions as a anti-viral protein during HBV infection by specifically inducing type interferon and some downstream antiviral effectors. This study is the first to report the application of iTRAQ technology to analyze the underlying mechanisms of HBV replication. Many of the differentially expressed proteins identified have not been linked to HBV replication before, and may provide valuable novel insights into HBV replication. J. Cell. Biochem. 114: 162–173, 2013.

KEY WORDS: HEPATITIS B VIRUS; HSPB1; iTRAQ

Hepatitis B virus (HBV) is the most common of the hepatitis viruses that cause chronic liver infections in humans. HBV infection is recognized as a major global health problem with an estimated two billion people infected with HBV worldwide, more than 350 million of whom have chronic liver infections [Lai et al., 2003]. Epidemiological studies of hepatitis B infection have revealed that it is a major cause of chronic hepatitis, liver fibrosis, and hepatocellular carcinoma (HCC). Each year over 1 million persons die from HBV-related liver diseases, 30–50% of which are attributed to HCC [Wright, 2006].

Hepatitis B is highly endemic in China, and is associated with up to 80–90% of the diagnosed HCC cases. Unfortunately, licensed treatments for HBV infection, which include interferon (IFN)-α, nucleoside (lamivudine) and nucleotide (adefovir) analogues, are capable of producing a long-term response in only a minority of the patients. Thus, it is critical to obtain a better understanding of the molecular mechanisms underlying HBV viral replication and infection pathogenesis.

Although the mechanism for reverse transcription (RT) in hepatitis B viruses is well understood, the impact of HBV replication on host gene and protein expression remains elusive. Over the past decades, many global gene and protein expression studies have been conducted in attempts to identify novel HBV-associated HCC diagnostic or prognostic markers that will differentiate between HBV-infected normal and tumor tissues. Using two-dimensional gel electrophoresis (2-DE), Lee et al. [2006] demonstrated that enhanced expression of the NF-kappa B-associated Wnt-1 protein might be a mechanism of hepatocarcinogenesis common to both HBV and hepatitis C virus (HCV) infections. Exploiting the recent advances in and availability of systems biology approaches, Lu et al. identified up-regulation of five common regulator genes in hepatitis B virus X protein (HBx)-expressing transgenic mouse, including EDN1, BMP7, BMP4, SPIB, and SRC. This trend correlated well with the progression of human liver cancer, and these [Feng et al., 2005] five regulators were proposed as potentially useful molecular targets for early-stage diagnosis or therapy of HCC [Lu et al., 2012].

*Correspondence to: Da-Zhi Zhang, Key Laboratory of Molecular Biology for Infectious Diseases of Ministry of Education of China, the Second Affiliated Hospital, Chongqing Medical University, Chongqing, China
E-mail: dzhzhang@yahoo.com

Manuscript Received: 13 May 2012; Manuscript Accepted: 30 July 2012
Accepted manuscript online in Wiley Online Library (wileyonlinelibrary.com): 8 August 2012
DOI 10.1002/jcb.24313 • © 2012 Wiley Periodicals, Inc.

2-DE is the principal step of proteomic-based approaches, and has been widely used in comparative studies of protein expression levels. However, this technique has several disadvantages, including poor reproducibility between gels, low sensitivity for detecting proteins at low concentrations and hydrophobic membrane proteins, limited sample capacity, and low linear visualization range [Gorg et al., 2000, 2004]. Over the past 5 years there has been an increasing interest in applying isotope-based quantitative proteomics in diverse research fields – ranging from biomarker discovery to post-translational modifications. The most recent technologies that have emerged include isotope-coded affinity tags (ICAT), isobaric tags for relative and absolute quantitation (iTRAQ), ^{18}O-labeling, and stable isotope labeling with amino acids in cell culture (SILAC) [Gygi et al., 1999; Mirgorodskaya et al., 2000; Ross et al., 2004]. Among these, the iTRAQ method is considered a particularly powerful tool since it can facilitate simultaneous analysis of up to eight samples in a single experiment.

In the current study, we employed iTRAQ to identify alterations in the proteome of HBV DNA-transfected HepG2.2.15 cells as compared to the parental cell line, HepG2. Using iTRAQ-coupled 2D liquid chromatography tandem mass-spectrophotometry (LC-MS/MS), an ultrasensitive proteomics platform, we successful identified 2,028 of human liver proteins from microgram amounts of starting material. In addition, our approach led to the identification of heat shock protein 27 (HSPB1), which was found to be highly expressed in the HBV-infected HepG2.2.15 and to interfere with HBV replication through the IFN signaling pathway.

MATERIALS AND METHODS

CELL LINES AND TISSUE SAMPLES

HepG2 and HepG2.2.15 cells were purchased from the American Type Culture Collection (Rockville, MD). Both cell lines were cultured in Dulbecco's Modified Eagle's Medium (DMEM; Gibco, San Diego, CA) supplemented with 10% fetal bovine serum (Hyclone, Logan, UT) at 37°C in an atmosphere containing 5% CO_2. Non-tumor liver tissue samples used for tissue microarray were collected from 90 HBV-associated HCC patients and 70 non-HBV HCC patients who underwent hepatectomy at the Second Affiliated Hospital of Chongqing Medical University. All patients were verified negative for human immunodeficiency virus (HIV) and hepatitis virus C (HCV). Approval from the Institutional Research Board at the Chongqing Medical University was obtained prior to the study.

REAGENTS

The iTRAQ kits were purchased from Applied Biosystems (Foster City, CA). Sequence-grade modified trypsin was purchased from Promega (Madison, WI). Polyvinylidene fluoride (PVDF) membrane, IgG antibodies (goat anti-mouse, goat anti-rabbit or rabbit anti-goat) conjugated with horseradish peroxidase (HRP), and the enhanced chemiluminescence (ECL) system were purchased from Amersham Biosciences (Uppsala, Sweden). Monoclonal antibodies against FABP1, ACAT2, ACY1, KRT19, HSPB1, and actin were from Abcam (Cambridge, MA). Specific siRNA oligonucleotides directed against human HSPB1 (SignalSilence® HSPB1 siRNA I #6356; SignalSilence® HSPB1 siRNA II #6526) were purchased from Cell Signaling Technology (Danvers, MA). Lipofectamine2000 was purchased from Invitrogen Life Technologies (Carlsbad, CA).

PROTEIN SAMPLE PREPARATION AND iTRAQ LABELING

Total protein extracts were prepared by the Sample Grinding Kit from Amersham Biosciences using the lysis buffer (7 M urea, 1 mg/ml DNase I, 1 mM Na_3VO_4, and 1 mM PMSF) and separated by centrifugation at 15,000 rpm for 30 min at 4°C. The supernatant was collected and the concentration of the total proteins was determined by the 2D Quantification Kit from Amersham Biosciences. From each cell line, 100 μg of proteins were acetone precipitated overnight at −20°C and dissolved in the lysis buffer, denatured, and treated for cysteine blocking as described in the iTRAQ protocol (Applied Biosystems). Each sample was digested with 20 μl of 0.1 μg/μl trypsin solution (Promega) at 37°C overnight and then labeled with the iTRAQ tags as follows: (i) HepG2: 113 and 115 tags; (ii) HepG2.2.15: 114 and 116 tags. The labeled samples were pooled prior to further analysis.

STRONG CATION EXCHANGE CHROMATOGRAPHY

To reduce the sample complexity for LC-MS/MS analysis, the pooled samples were diluted 10-fold with SCX buffer A (10 mM KH_2PO_4 in 25% acetonitrile at pH 3.0) and applied to a 2.1 × 200 mm polysulfoethyl A SCX column (Poly LC, Columbia, MD). The column was eluted with a gradient of 0–25% SCX buffer B (10 mM KH_2PO_4 at pH 3.0 in 25% acetonitrile containing 350 mM KCl) over 30 min, followed by a gradient of 25–100% SCX buffer B over 40 min. Fractions were collected at 1 min intervals. These SCX fractions were lyophilized in a vacuum concentrator, and subjected to C-18 clean-up using a C18 Discovery® DSC-18 SPE column (100 mg capacity; Supelco; Sigma–Aldrich, St. Louis, MO). The cleaned fractions were then lyophilized again and stored at −20°C until use in mass spectrometric analysis.

MASS SPECTROMETRIC ANALYSIS

Mass spectrometric analysis was performed using a nano-LC coupled online to a QStar Elite mass spectrometer (Applied Biosystems). Peptides were loaded on a 75 μm × 15 cm, 3 μm fused silica C-18 capillary column, followed by a mobile phase elution with buffer A (0.1% formic acid in 2% acetonitrile) and buffer B (0.1% formic acid in 98% acetonitrile). The peptides were eluted from 2% buffer B to 100% buffer B over 60 min at a flow rate of 300 nL/min. The LC eluent was directed to the electrospray (ESI) source for quadrupole-time of flight (Q-TOF)-MS analysis. The mass spectrometer was set to perform information-dependent acquisition (IDA) in the positive ion mode, with a selected mass range of 300–2,000 m/z. Peptides with +2 to +4 charge states were selected for tandem mass spectrometry, and the time of summation of MS/MS events was set to 3 s. The two most abundantly charged peptides above a 10-count threshold were selected for MS/MS and dynamically excluded for 60 s with ±50 mmu mass tolerance.

Peptide identification and quantification were performed using ProteinPilot software packages (Applied Biosystems). Each MS/MS spectrum was searched against the international protein index (IPI) human protein database v3.49, and protein identification was accepted based on ProteinPilot confidence scores. Relative

quantification of proteins, in the case of iTRAQ, was performed on the MS/MS scans and was defined as the ratio of the areas under the peaks at 113, 114, 115, and 116 Da, which were the masses of the tags that corresponded to the iTRAQ reagents. The error factor (EF) and *P*-value were calculated by the ProteinPilot software, each of which gave an indication of the deviation and significance in the protein quantification.

REAL-TIME QUANTITATIVE RT-PCR ANALYSIS

Total RNA was extracted using the Trizol reagent (Gibco BRL, Gaithersburg, MD) and following the manufacturer's instructions. Two micrograms of total RNA was reverse-transcribed into first-strand cDNA using the A3500 Reverse Transcription System (Promega) Quantitative RT-PCR was performed on the ABI 7900HT System using the TaqMan GeneExpression Assay Kit and gene-specific primers for 18S (Hs99999901_s1), KRT19 (Hs00761767_s1), HSPB1 (Hs03044127_g1), PA2G4 (Hs00854538_g1), RUVBL2 (Hs01090542_m1), DNAJB1 (Hs00428680_m1), SFRS9 (Hs01596548_g1), BLVRA (Hs00167599_m1), SFN (Hs00968567_s1), SOD1 (Hs00533490_m1), VAT1 (Hs00197262_m1), HSPA5 (Hs00607129_gH), and PCK2 (Hs00388934_m1). To detect the expression levels of type I IFN and the downstream IFN-stimulated genes triggered by HSPB1 over-expression, gene-specific primers for IFNα1 (Hs00855471_g1), IFNβ1 (Hs01077958_s1), ISG15 (Hs01921425_s1), Mx1 (Hs00895608_m1), OAS1 (Hs00973637_m1), OAS2 (Hs00942643_m1), OAS3 (Hs00196324_m1), OASL (Hs00984390_m1), PKR (Hs00169345_m1), and EIF2α (Hs00230684_m1) were used. The relative quantification of gene expression was analyzed using the $2^{-\Delta\Delta CT}$ method [Livak and Schmittgen, 2001]. Real-time quantitative RT-PCR analysis was repeated atleast three times.

WESTERN BLOTTING ANALYSIS

The cells were lysed at 4°C for 30 min in lysis buffer (50 mM Tris, pH 7.4, 100 mM NaCl, 1 mM $MgCl_2$, 2.5 mM Na_3VO_4, 1 mM PMSF, 2.5 mM EDTA, 0.5% Triton X-100, 0.5% NP-40, and 5 μg/ml each of aprotinin, pepstatin A and leupeptin). The lysates were centrifuged at 15,000 rpm for 15 min at 4°C. Protein concentration was determined using the 2D Quantification Kit (Amersham Biosciences). The protein samples (~20 μg) were separated by SDS–PAGE and transferred to PVDF membranes. The membranes were blocked overnight at 4°C with 5% non-fat dry milk in TBS-T buffer (20 mM Tris, pH 7.6, 100 mM NaCl, 0.5% Tween-20), followed by 3 h of incubation with the primary antibody (1:1,500–1:2,000 dilution) in TBS-T buffer containing 5% non-fat dry milk at room temperature. After washing three times with TBS-T buffer, the membranes were incubated with an HRP-conjugated goat anti-mouse IgG, goat anti-rabbit IgG, or rabbit anti-goat IgG as the secondary antibody (1:3,000 dilution) for 1 h at room temperature. The membranes were then washed three times in TBS-T buffer and the reactions were visualized with the ECL detection system. All of the Western blotting analyses were repeated at least three times.

PLASMIDS AND TRANSFECTIONS

The full-length cDNA for human HSPB1 was subcloned into the PCMV-tag2B vector at the *Bam*HI and *Xho*I sites. Two vectors were created for study: PCMV-tag2B-hHSPB1 andPCMV-tag2B (empty vector). Clone identity was verified using restriction digest analysis and plasmid DNA sequencing. HepG2.2.15 cells were transfected with HSPB1 vector and targeting siRNA using Lipofectamine2000 and following the manufacturer's protocol. Cells were harvested 2 days after transfection for Western blot analysis. Transfection efficiency was 65% (data not shown).

SUPERNATANT HBV DNA ANALYSIS

Culture mediums were collected for quantification of HBV DNA. Brief centrifugation was used to remove cell debris. Viral core particles were precipitated with 10% polyethylene glycol 8000 in 0.5 M NaCl at 4°C overnight. After centrifugation at 15,000 rpm for 30 min, viral cores were pelleted and subsequently treated with DNase I (100 μg/ml in 50 mM Tris–HCl, pH 8.0, 10 mM $MgCl_2$) at 37°C for 3 h. The mixture was further digested with proteinase K (400 μg/ml in 15 mM EDTA, 100 mM NaCl, 0.5% SDS) at 55°C for 2 h, which was followed by phenol/chloroform extraction. HBV DNA was ethanol precipitated, resuspended in TE buffer (10 mM Tris–HCl, pH 8.0, 1 mM EDTA) and digested with 100 ng/μl of RNase A for 30 min at 37°C. Purified DNA was then subjected to HBV DNA quantification using real-time RT-PCR. Levels of hepatitis B surface antigen (HBsAg) and hepatitis B e antigen (HBeAg) in the media of the transfected cells were determined by enzyme-linked immunosorbent assay (ELISA).

IMMUNOHISTOCHEMISTRY (IHC) AND TISSUE MICROARRAY

Two candidate proteins, HSPB1 and KRT19, were selected for further analysis by tissue microarray based on the fact that they had not been previously reported as aberrantly expressed in hepatitis B patients. Briefly, paraffin-embedded human liver sections were warmed in a 60°C oven, dewaxed by three soakings in xylene, and passaged through a graded ethanol series (100, 95, and 70%) before a final wash in double-distilled H_2O. After quenching of endogenous peroxidase activity with 3% H_2O_2 for 10 min and blocking with bovine serum albumin (BSA) for 30 min, sections were incubated at 4°C overnight with antibodies against HSPB1 (1:2,000) and KRT19 (1:2,000). Detection was achieved with the Envision HRP System (Dako-Cytomation, Glostrup, Denmark). All slides were counter-stained with Gill's hematoxylin for 1 min, dehydrated, and mounted for light microscope evaluation. Protein expression was assessed using a semi-quantitative scoring method that consisted of an assessment for both staining intensity (scale: 0 to 3) and the percentage of positive cells (0 to 100%), which, when multiplied, generated a score ranging from 0 to 300. Interpretation of hematoxylin and eosin-stained sections and analysis/scoring of the TMA data were all carried out by a single certified pathologist to maintain consistency.

STATISTICAL ANALYSIS

Statistical analysis was carried out with the SPSS v10.0 software for Windows (SPSS Inc., Chicago, IL). The data are expressed as mean ± SD. Between-group comparisons were carried out with the Student's *t*-test at 95% confidence. Statistical significance was indicated by *P*-value <0.05.

RESULTS

iTRAQ ANALYSIS OF DIFFERENTIALLY EXPRESSED PROTEINS

To investigate the molecular characteristics of HBV replication, we employed a quantitative proteomic approach with isobaric labeling (iTRAQ) using the HepG2.2.15 cell line and its parental cell line, HepG2. To increase the coverage of protein identification and/or the confidence of the data generated, samples were iTRAQ labeled in duplicate as follows (100 μg each per label): HepG2, 113; HepG2, 115; HepG2.2.15, 114; HepG2.2.15, 116. To reduce the extreme complexity of the sample, a batch of 70 fractions per iTRAQ experiment was separated using strong cation exchange chromatography. These fractions were then combined in 20 samples and analyzed by LC/MS/MS. A schematic flowchart of the iTRAQ method is shown in Fig. 1A. The MS/MS spectrum of HSPB1 (peptide sequence: LATQSNEITIPVTFESR) is presented in Fig. 1B. HepG2.2.15 cells were labeled with iTRAQ 114 and 116 tags, and HepG2 cells were labeled with iTRAQ 113 and 115 tags. Thus, the ratio of 116:115 and 114:113 indicated the relative abundance of HSPB1 protein (Fig. 1B) in HepG2.2.15 cells compared to that in HepG2 cells. When the same protein gave two relative quantitative ratios in both 116:115 and 114:113, the quantitation ratio from the experiment with the best *P*-values was selected. A total of 2,028 unique proteins was identified with 95% confidence. Although the

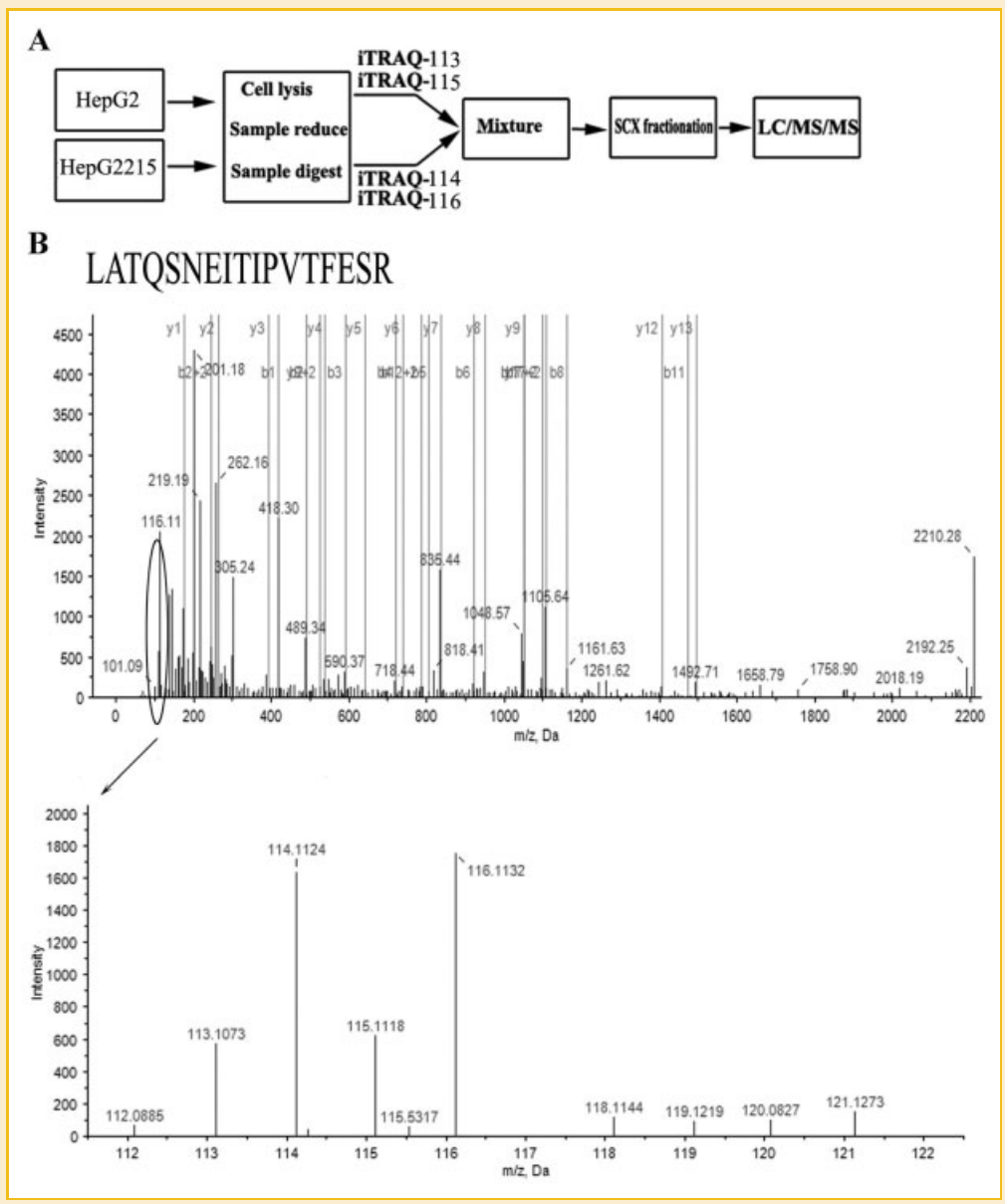

Fig. 1. A: Flowchart of the iTRAQ proteomics approach used in this study. B: Representative MS/MS spectrum showing the peptides from HSPB1 (peptide sequence: LATQSNEITIPVTFESR). HepG2.2.15 cells were labeled with iTRAQ 114 and 116 tags, and HepG2 cells were labeled with iTRAQ 113 and 115 tags. Thus, the ratio of 116:115 and 114:113 indicated the relative abundance of the HSPB1 protein in HepG2.2.15 compared to HepG2.

relative quantification analysis by ProteinPilot 2.0 software is generated by statistical analysis and since most methods are prone to technical variation, we included an additional 1.3-fold change cutoff for all iTRAQ ratios in order to reduce false positives for the selection of differentially expressed proteins. This filtering measure resulted in a final set of 170 proteins differentially expressed between HepG2.2.15 and HepG2 cells (Table I). These 170 proteins were classified into 21 functional categories by using the PANTHER classification system (www.pantherdb.org) (Fig. 2). The top four molecular functions categories were oxidoreductase (15.1%), nucleic acid binding (13.8%), transferase (11.6%), hydrolase (7.1%).

VALIDATION OF DIFFERENTIALLY EXPRESSED PROTEINS

The differential expression levels of the proteins identified by the iTRAQ approach were validated by using real-time quantitative RT-PCR analysis and Western blotting. Fig. 3A shows the relative mRNA expression levels of KRT19, PA2G4, RUVBL2, DNAJB1, SFRS9, BLVRA, SFN, HSPB1, SOD1, VAT1, HSPA5, and PCK2 normalized with 18S rRNA. The mRNA levels of KRT19, PA2G4, RUVBL2, DNAJB1, SFRS9, BLVRA, SFN, and HSPB1 were up-regulated in 'HepG2.2.15 cells, whereas the mRNA levels of SOD1, VAT1, HSPA5, and PCK2 were down-regulated, as compared to HepG2 cells. This trend was similar to the protein expression level determined by the iTRAQ approach. Fig. 3B shows a representative Western blot analysis result of HSPB1, KRT19, FABP1, ACAT2, and ACY1 expression in the two cell lines. Compared with HepG2, HepG2.2.15 had an obvious up-regulation of HSPB1 and KRT19, and a marked down-regulation of FABP1, ACAT2, and ACY1.

RELEVANCE OF ABERRANT HSPB1 EXPRESSION IN CLINICAL SAMPLES

The corresponding non-tumor normal tissues of 160 HCC patients that were negative or positive for HBV markers were used to create the tissue microarrays. The ages of these patients ranged from 25 to 98 years old, and the majority of the cohort (77%) was male. The grade and stage of most non-tumor tissues (71%) indicated liver cirrhosis. Representative images of the IHC results for HSPB1 and KRT19 in HBV(+) and HBV(−) liver tissues are shown in Fig. 4A. The results showed that the highest levels of signal intensity were detected in specimens from HBV(+) tissues. As shown in Fig. 4B, IHC score values of HSPB1 and KRT19 were significantly higher in HBV(+) tissues than in HBV(−) tissues. HSPB1, for example, was detected in 121/160 (75.6%) cases of HBV(+) HCC with IHC scores >50, and only in 43/160 (26.9%) cases of HBV(−) HCC tissues.

ASSOCIATION OF HSPB1 WITH HBV REPLICATION

To study the functional role of HSPB1 up-regulation in HepG2.2.15, HSPB1 expression was silenced with siRNA. As shown by Western blotting, HSPB1 siRNA transfection of HepG2.2.15 cells significantly reduced HSPB1 protein levels, whereas control siRNA did not produce a significant effect on HSPB1 protein expression. We next tested the effect of HSPB1 siRNA transfection on HBV replication. After 48 h of incubation, the HSPB1 siRNA-transfected HepG2.2.15 cells showed enhanced HBV DNA, HBsAg and HBeAg levels. The increase in HBV DNA production was almost a 2-fold higher than in the controls (Fig. 5A). Furthermore, transfection of the HepG2.2.15 cells with a HSPB1-expression vector led to a marked decrease in HBV replication, and the levels of HBsAg and HBeAg in the culture medium were significantly decreased (Fig. 5B). The above results indicated that HSPB1 can act as an endogenous anti-HBV factor that interferes with HBV production.

HSPB1-MEDIATED ALTERATION OF IFN-INDUCED DOWNSTREAM SIGNALING PATHWAYS

We detected the expression levels of type I IFN and downstream IFN-stimulated genes in response to HSPB1 overexpression. As shown in Fig. 5C, transfection of the HSPB1-expression vector caused increased mRNA levels of type I IFN and five downstream IFN-stimulated genes (ISG15, OAS1, OAS3, PKR, and EIF2α). However, three other effectors of the type I IFN-mediated antiviral signal, Mx1, OAS2, and OASL, showed only minimally altered mRNA levels in response to HSPB1 overexpression.

DISCUSSION

Chronic HBV infection not only results in fatal liver diseases, such as cirrhosis and liver failure, but also dramatically increases the risk of liver cancer by over 100-fold. Understanding the molecular mechanisms of HBV replication and infection pathogenesis are key measures to not only to improve patient screening and treatment regimens but also to provide new avenues for drug and vaccine development. In this study, we used the iTRAQ proteomic approach to identify proteins with differential expression between HBV DNA-expressing HepG2.2.15 and the parental cell line, HepG2. As a result, 170 proteins were found with significant alterations in expression between the two cell lines. Many of them, including KRT19, PA2G4, RUVBL2, DNAJB1, SFRS9, BLVRA, SFN, HSPB1, and SOD1, were confirmed using real-time RT-PCR analysis and Western blot analysis. In addition, IHC on tissue microarray demonstrated the up-regulation of HSPB1 and KRT19 expression in HBV-infected patients. Collectively, these data provide evidence that the iTRAQ reagents labeling method for large scale protein quantification is powerful and reliable for in vitro and in vivo HBV-related investigations. Based on the PANTHER classification system, all 170 proteins were classified into 21 functional categories. We discuss some of the key proteins discovered in this work in the following text.

The expression levels of HSPB1 were found to be significantly increased not only in the HBV DNA-transfected HepG2.2.15 cell line but also in HBV(+) human liver tissue samples, as compared with their non-HBV counterparts. These findings indicate an association between HSPB1 and HBV infection, which is supported by previous findings in the literature. While HSPB1 expression was reported as low or non-detectable in liver tissues of patients with HBV infection [Ciocca et al., 1991], up-regulated HSPB1 was found to be frequently detected in clinical samples (serum and liver tissue) of HCC patients [Feng et al., 2005; Lim et al., 2005]. A link between HSPB1 expression and subsequent onset of HBV-related HCC and other life-threatening complications was demonstrated by Harimoto et al. In that study, high expression of HSPB1 was shown to be significantly associated with poor prognosis in patients with HBV infection but

TABLE I. iTRAQ Analysis of Differentially Expressed Proteins Between HepG2.2.15 and HepG2

Number	Accession	Gene	Protein	HepG2.2.15: HepG2	PVal (HepG2.2.15: HepG2)
1	IPI:IPI00010290.2	FABP1	FABP1 protein (Fragment)	0.24	3.44E-03
2	IPI:IPI00296645.4	MTTP	Microsomal triglyceride transfer protein large subunit	0.34	1.50E-02
3	IPI:IPI00105407.1	AKR1B10	Aldo-keto reductase family 1 member B10	0.34	2.06E-02
4	IPI:IPI00011454.1	GANAB	Isoform 2 of Neutral alpha-glucosidase AB	0.36	2.57E-05
5	IPI:IPI00009268.2	ACY1	Aminoacylase-1	0.38	2.55E-02
6	IPI:IPI00746777.3	ADH5	Alcohol dehydrogenase class-3	0.39	1.96E-03
7	IPI:IPI00332371.9	PFKL	Isoform 1 of 6-phosphofructokinase, liver type	0.41	2.79E-02
8	IPI:IPI00291419.6	ACAT2	Acetyl-CoA acetyltransferase, cytosolic	0.42	1.10E-02
9	IPI:IPI00216456.5	HIST1H2AC	Histone H2A type 1-C	0.42	1.70E-03
10	IPI:IPI00294380.5	PCK2	Phosphoenolpyruvate carboxykinase [GTP], mitochondrial	0.45	1.21E-04
11	IPI:IPI00011274.3	HNRPDL	Isoform 1 of Heterogeneous nuclear ribonucleoprotein D-like	0.46	1.26E-02
12	IPI:IPI00872692.1	QPRT	34 kDa protein	0.47	4.21E-02
13	IPI:IPI00217872.3	PGM1	Isoform 2 of Phosphoglucomutase-1	0.47	1.39E-02
14	IPI:IPI00619966.1	NQO1	NAD(P)H menadione oxidoreductase 1, dioxin-inducible isoform b	0.47	1.34E-11
15	IPI:IPI00156689.3	VAT1	Synaptic vesicle membrane protein VAT-1 homolog	0.47	2.97E-02
16	IPI:IPI00642549.2	RAD23B	UV excision repair protein RAD23 homolog B	0.48	1.38E-02
17	IPI:IPI00219897.1	ACSL4	Isoform Short of Long-chain-fatty-acid--CoA ligase 4	0.48	4.03E-02
18	IPI:IPI00016610.2	PCBP1	Poly(rC)-binding protein 1	0.48	3.84E-04
19	IPI:IPI00298406.3	HADH	Isoform 2 of Hydroxyacyl-coenzyme A dehydrogenase, mitochondrial	0.48	4.62E-02
20	IPI:IPI00292135.1	LBR	Lamin-B receptor	0.50	3.33E-02
21	IPI:IPI00171438.2	TXNDC5	Thioredoxin domain-containing protein 5	0.50	6.57E-10
22	IPI:IPI00797917.1	DCXR	DCXR 26 kDa protein	0.50	8.97E-05
23	IPI:IPI00921118.1	ACTN1	Actinin alpha 1 isoform 3	0.52	1.42E-02
24	IPI:IPI00218733.6	SOD1	Superoxide dismutase [Cu-Zn]	0.52	1.23E-03
25	IPI:IPI00031661.1	NOC4L	Nucleolar complex protein 4 homolog	0.53	7.23E-03
26	IPI:IPI00003704.4	RBM4	Isoform 1 of RNA-binding protein 4	0.53	4.56E-02
27	IPI:IPI00551024.4	DAK	Dihydroxyacetone kinase	0.53	2.74E-05
28	IPI:IPI00040900.3	HS2ST1	Isoform 2 of Heparan sulfate 2-O-sulfotransferase 1	0.53	3.10E-02
29	IPI:IPI00921830.1	DBI	Diazepam binding inhibitor, splice form 1D	0.53	6.27E-03
30	IPI:IPI00026781.2	FASN	Fatty acid synthase	0.53	2.46E-15
31	IPI:IPI00027223.2	IDH1	Isocitrate dehydrogenase [NADP] cytoplasmic	0.54	9.69E-06
32	IPI:IPI00152432.2	GPT2	Isoform 1 of Alanine aminotransferase 2	0.55	2.91E-03
33	IPI:IPI00005202.2	PGRMC2	Membrane-associated progesterone receptor component 2	0.55	1.75E-02
34	IPI:IPI00395998.5	RPL32	60S ribosomal protein L32	0.57	2.01E-02
35	IPI:IPI00847322.1	SOD2	manganese superoxide dismutase isoform A precursor	0.57	2.95E-04
36	IPI:IPI00021812.2	AHNAK	Neuroblast differentiation-associated protein AHNAK	0.58	9.49E-19
37	IPI:IPI00009896.1	EPHX1	Epoxide hydrolase 1	0.58	1.01E-02
38	IPI:IPI00646304.4	PPIB	Peptidyl-prolyl cis-trans isomerase B	0.58	7.20E-06
39	IPI:IPI00641334.2	CYB5B	Cytochrome b5 type B	0.59	9.04E-03
40	IPI:IPI00607801.2	CES1	Isoform 2 of Liver carboxylesterase 1	0.59	1.42E-04
41	IPI:IPI00030207.1	GMDS	GDP-mannose 4,6 dehydratase	0.60	4.07E-02
42	IPI:IPI00003362.2	HSPA5	HSPA5 protein	0.61	2.20E-13
43	IPI:IPI00010796.1	P4HB	Protein disulfide-isomerase	0.61	8.08E-21
44	IPI:IPI00216457.7	HIST2H2AA4	Histone H2A type 2-A	0.62	1.12E-03
45	IPI:IPI00011200.5	PHGDH	D-3-phosphoglycerate dehydrogenase	0.62	9.60E-04
46	IPI:IPI00643920.3	TKT	Transketolase	0.63	3.84E-05
47	IPI:IPI00001734.3	PSAT1	Phosphoserine aminotransferase	0.63	1.99E-04
48	IPI:IPI00479185.1	TPM3	tropomyosin 3 isoform 4	0.63	4.65E-02
49	IPI:IPI00020599.1	CALR	Calreticulin	0.64	1.62E-09
50	IPI:IPI00894154.1	NDUFA10	NADH dehydrogenase ubiquinone 1 alpha subcomplex	0.65	1.71E-02
51	IPI:IPI00022463.1	TF	Serotransferrin	0.65	6.43E-04
52	IPI:IPI00026519.1	PPIF	Peptidyl-prolyl cis-trans isomerase, mitochondrial	0.65	1.05E-02
53	IPI:IPI00783987.2	C3	Complement C3 (Fragment)	0.66	3.31E-02
54	IPI:IPI00025252.1	PDIA3	Protein disulfide-isomerase A3	0.66	5.76E-06
55	IPI:IPI00022228.2	HDLBP	Vigilin	0.66	5.34E-03
56	IPI:IPI00026530.4	LMAN1	Protein ERGIC-53	0.66	4.55E-02
57	IPI:IPI00024466.2	UGCGL1	Isoform 1 of UDP-glucose:glycoprotein glucosyltransferase 1	0.66	3.08E-02
58	IPI:IPI00792395.2	POR	Putative uncharacterized protein DKFZp686G04235	0.67	1.41E-02
59	IPI:IPI00009904.1	PDIA4	Protein disulfide-isomerase A4	0.67	9.30E-05
60	IPI:IPI00218693.8	APRT	Adenine phosphoribosyltransferase	0.67	2.31E-02
61	IPI:IPI00477729.2	ACOX1	Isoform 2 of Peroxisomal acyl-coenzyme A oxidase 1	0.68	5.61E-03
62	IPI:IPI00024623.3	ACADSB	Short/branched chain specific acyl-CoA dehydrogenase, mitochondrial	0.68	2.23E-02
63	IPI:IPI00297084.7	DDOST	dolichyl-diphosphooligosaccharide-protein glycosyltransferase precursor	0.68	1.02E-02
64	IPI:IPI00303300.3	FKBP10	FK506-binding protein 10	0.69	4.10E-03
65	IPI:IPI00871932.1	SPTBN1	276 kDa protein	0.69	3.50E-04
66	IPI:IPI00030275.5	TRAP1	Heat shock protein 75 kDa, mitochondrial	0.70	1.85E-02
67	IPI:IPI00604710.2	SLC3A2	solute carrier family 3 (activators of dibasic and neutral amino acid transport), member 2 isoform c	0.70	2.76E-02
68	IPI:IPI00877938.1	IARS	isoleucyl-tRNA synthetase	0.71	1.53E-02
69	IPI:IPI00031420.3	UGDH	UDP-glucose 6-dehydrogenase	0.71	1.06E-07
70	IPI:IPI00102896.1	RAB2B	Ras-related protein Rab-2B	0.71	1.12E-02
71	IPI:IPI00030363.1	ACAT1	Acetyl-CoA acetyltransferase, mitochondrial	0.72	1.45E-02
72	IPI:IPI00553185.2	CCT3	T-complex protein 1 subunit gamma	0.72	1.60E-03
73	IPI:IPI00218235.5	DHRS2	dehydrogenase/reductase member 2 isoform 2	0.72	1.14E-08
74	IPI:IPI00005154.1	SSRP1	FACT complex subunit SSRP1	0.72	3.66E-02

(*Continued*)

TABLE I. (*Continued*)

Number	Accession	Gene	Protein	HepG2.2.15: HepG2	PVal (HepG2.2.15: HepG2)
75	IPI:IPI00025091.3	RPS11	40S ribosomal protein S11	0.73	3.13E-02
76	IPI:IPI00217465.5	HIST1H1C	Histone H1.2	0.74	1.00E-02
77	IPI:IPI00009923.1	P4HA1	Isoform 1 of Prolyl 4-hydroxylase subunit alpha-1	0.75	4.84E-03
78	IPI:IPI00844076.1	RPN2	Dolichyl-diphosphooligosaccharide--protein glycosyltransferase subunit 2	0.75	6.99E-03
79	IPI:IPI00419373.1	HNRNPA3	Isoform 1 of Heterogeneous nuclear ribonucleoprotein A3	0.75	7.82E-03
80	IPI:IPI00419979.3	PAK2	Serine/threonine-protein kinase PAK 2	0.75	9.82E-03
81	IPI:IPI00604620.3	NCL	Nucleolin	0.75	1.56E-04
82	IPI:IPI00304612.9	RPL13A	60S ribosomal protein L13a	0.75	4.34E-02
83	IPI:IPI00604590.3	NME2	Nucleoside diphosphate kinase	0.76	1.76E-05
84	IPI:IPI00394838.3	ACLY	ATP-citrate synthase	0.76	4.49E-03
85	IPI:IPI00796333.1	ALDOA	45 kDa protein	0.77	2.66E-09
86	IPI:IPI00002520.1	SHMT2	Serine hydroxymethyltransferase, mitochondrial	0.77	4.06E-03
87	IPI:IPI00292020.3	SRM	Spermidine synthase	1.31	3.57E-02
88	IPI:IPI00465248.5	ENO1	Isoform alpha-enolase of Alpha-enolase	1.32	7.28E-12
89	IPI:IPI00784044.1	MCCC2	Isoform 1 of Methylcrotonoyl-CoA carboxylase beta chain, mitochondrial	1.32	2.33E-02
90	IPI:IPI00383046.3	CMBL	Carboxymethylenebutenolidase homolog	1.33	3.32E-02
91	IPI:IPI00219018.7	GAPDH	Glyceraldehyde-3-phosphate dehydrogenase	1.33	2.17E-14
92	IPI:IPI00878611.1	RANBP1	29 kDa protein	1.33	2.50E-02
93	IPI:IPI00015911.1	DLD	Dihydrolipoyl dehydrogenase, mitochondrial	1.34	3.22E-03
94	IPI:IPI00792100.1	CLE	C14orf166	1.34	4.16E-02
95	IPI:IPI00179330.6	UBB	UBC ubiquitin and ribosomal protein S27a precursor	1.34	3.56E-03
96	IPI:IPI00298547.3	PARK7	Protein DJ-1	1.35	1.93E-02
97	IPI:IPI00169383.3	PGK1	Phosphoglycerate kinase 1	1.35	1.11E-04
98	IPI:IPI00219616.7	PRPS1	Ribose-phosphate pyrophosphokinase 1	1.36	4.55E-02
99	IPI:IPI00002966.2	HSPA4	Heat shock 70 kDa protein 4	1.36	8.31E-03
100	IPI:IPI00647268.1	RHOC	Ras homolog gene family, member C	1.36	2.51E-02
101	IPI:IPI00792352.1	RAN	26 kDa protein	1.36	4.30E-03
102	IPI:IPI00013933.2	DSP	Isoform DPI of Desmoplakin	1.37	2.78E-03
103	IPI:IPI00300074.3	FARSB	Phenylalanyl-tRNA synthetase beta chain	1.38	2.35E-02
104	IPI:IPI00141318.2	CKAP4	Isoform 1 of Cytoskeleton-associated protein 4	1.39	2.42E-02
105	IPI:IPI00304171.6	H2AFY	Isoform 2 of Core histone macro-H2A.1	1.40	1.64E-02
106	IPI:IPI00011107.2	IDH2	Isocitrate dehydrogenase [NADP], mitochondrial	1.40	4.32E-02
107	IPI:IPI00792916.2	PRKCSH	protein kinase C substrate 80K-H isoform 2	1.40	6.35E-03
108	IPI:IPI00171611.7	HIST2H3A	Histone H3.2	1.40	2.45E-02
109	IPI:IPI00004860.2	RARS	Isoform Complexed of Arginyl-tRNA synthetase, cytoplasmic	1.41	3.70E-02
110	IPI:IPI00795979.1	FLOT2	Flotillin-2	1.41	4.59E-02
111	IPI:IPI00009950.1	LMAN2	Vesicular integral-membrane protein VIP36	1.41	4.16E-02
112	IPI:IPI00219446.5	PEBP1	Phosphatidylethanolamine-binding protein 1	1.42	1.23E-03
113	IPI:IPI00645078.1	UBA1	Ubiquitin-like modifier-activating enzyme 1	1.43	3.93E-03
114	IPI:IPI00307155.7	ROCK2	Rho-associated protein kinase 2	1.43	4.81E-02
115	IPI:IPI00006663.1	ALDH2	Aldehyde dehydrogenase, mitochondrial	1.43	2.43E-02
116	IPI:IPI00216654.2	NOLC1	Isoform Beta of Nucleolar phosphoprotein p130	1.43	9.04E-03
117	IPI:IPI00844361.1	RAB18	RAB18 long isoform 1	1.43	1.97E-02
118	IPI:IPI00745502.2	PSMC5	Proteasome (Prosome, macropain) 26S subunit, ATPase, 5, isoform CRA_b	1.43	5.51E-03
119	IPI:IPI00384857.3	HN1	Isoform 2 of Hematological and neurological expressed 1 protein	1.43	1.65E-02
120	IPI:IPI00028520.2	NDUFV1	Isoform 1 of NADH dehydrogenase [ubiquinone] flavoprotein 1, mitochondrial	1.44	1.13E-02
121	IPI:IPI00031461.2	GDI2	Rab GDP dissociation inhibitor beta	1.45	1.51E-06
122	IPI:IPI00024993.4	ECHS1	Enoyl-CoA hydratase, mitochondrial	1.45	2.21E-02
123	IPI:IPI00291006.2	MDH2	Malate dehydrogenase, mitochondrial	1.45	9.24E-05
124	IPI:IPI00654777.2	EIF3F	HCG1784554, isoform CRA_a	1.45	1.66E-02
125	IPI:IPI00029764.1	SF3A3	Splicing factor 3A subunit 3	1.46	1.87E-02
126	IPI:IPI00103994.4	LARS	Leucyl-tRNA synthetase, cytoplasmic	1.46	1.94E-02
127	IPI:IPI00304435.3	NIPSNAP1	Protein NipSnap homolog 1	1.47	1.39E-02
128	IPI:IPI00003949.1	UBE2N	Ubiquitin-conjugating enzyme E2 N	1.47	4.70E-02
129	IPI:IPI00922603.1	MAOB	Amine oxidase (flavin-containing) B	1.48	3.31E-02
130	IPI:IPI00020984.2	CANX	Calnexin	1.49	6.78E-04
131	IPI:IPI00305383.1	UQCRC2	Cytochrome b-c1 complex subunit 2, mitochondrial	1.49	1.53E-02
132	IPI:IPI00911050.1	FDXR	NADPH:adrenodoxin oxidoreductase, mitochondrial	1.50	2.23E-02
133	IPI:IPI00550746.4	NUDC	Nuclear migration protein nudC	1.51	2.07E-02
134	IPI:IPI00218547.1	ALDH18A1	Isoform Short of Delta-1-pyrroline-5-carboxylate synthetase	1.51	1.65E-05
135	IPI:IPI00294158.1	BLVRA	Biliverdin reductase A	1.52	4.78E-02
136	IPI:IPI00235412.6	DNM1L	Dynamin-1-like protein	1.52	1.77E-02
137	IPI:IPI00293276.10	MIF	Macrophage migration inhibitory factor	1.52	5.24E-05
138	IPI:IPI00010415.2	ACOT7	Isoform 1 of Cytosolic acyl coenzyme A thioester hydrolase	1.52	3.93E-02
139	IPI:IPI00440703.1	GSTK1	glutathione S-transferase kappa 1 isoform b	1.53	4.48E-02
140	IPI:IPI00290142.5	CTPS	CTP synthase 1	1.57	5.83E-04
141	IPI:IPI00549248.4	NPM1	Isoform 1 of Nucleophosmin	1.58	8.57E-11
142	IPI:IPI00301263.2	CAD	CAD protein	1.59	7.73E-03
143	IPI:IPI00017726.1	HSD17B10	Isoform 1 of 3-hydroxyacyl-CoA dehydrogenase type-2	1.62	1.47E-02
144	IPI:IPI00015953.3	DDX21	Isoform 1 of Nucleolar RNA helicase 2	1.63	2.03E-02
145	IPI:IPI00294536.2	STRAP	Serine-threonine kinase receptor-associatedprotein	1.65	2.81E-02
146	IPI:IPI00023640.3	PDCD5	Programmed cell death protein 5	1.66	2.58E-02
147	IPI:IPI00219306.1	MAGOH	Protein mago nashi homolog	1.70	2.89E-02
148	IPI:IPI00015018.1	PPA1	Inorganic pyrophosphatase	1.70	1.15E-05

(*Continued*)

TABLE I. (*Continued*)

Number	Accession	Gene	Protein	HepG2.2.15: HepG2	PVal (HepG2.2.15: HepG2)
149	IPI:IPI00218568.7	PCBD1	Pterin-4-alpha-carbinolamine dehydratase	1.70	1.55E-02
150	IPI:IPI00299000.5	PA2G4	Proliferation-associated protein 2G4	1.70	1.54E-04
151	IPI:IPI00025366.4	CS	Citrate synthase, mitochondrial	1.71	8.20E-05
152	IPI:IPI00022095.3	PEG10	Isoform RF1/RF2 of Retrotransposon-derived protein PEG10	1.73	3.82E-03
153	IPI:IPI00872780.1	ANXA4	Annexin A4	1.76	6.13E-05
154	IPI:IPI00554788.5	KRT18	Keratin, type I cytoskeletal 18	1.76	1.01E-21
155	IPI:IPI00003865.1	HSPA8	Isoform 1 of Heat shock cognate 71 kDa protein	1.78	2.25E-02
156	IPI:IPI00007797.3	FABP5	Fatty acid-binding protein, epidermal	1.78	1.50E-02
157	IPI:IPI00554648.3	KRT8	Keratin, type II cytoskeletal 8	1.82	6.43E-10
158	IPI:IPI00009104.7	RUVBL2	RuvB-like 2	1.83	2.37E-03
159	IPI:IPI00000105.4	MVP	Major vault protein	1.89	4.82E-02
160	IPI:IPI00015947.5	DNAJB1	DnaJ homolog subfamily B member 1	1.92	2.76E-02
161	IPI:IPI00293242.1	GTF2I	Isoform 2 of General transcription factor II-I	1.94	7.55E-03
162	IPI:IPI00216230.3	TMPO	Lamina-associated polypeptide 2, isoform alpha	2.03	3.58E-02
163	IPI:IPI00646762.1	NUDT5	Putative uncharacterized protein NUDT5	2.09	1.88E-02
164	IPI:IPI00013890.2	SFN	Isoform 1 of 14-3-3 protein sigma	2.14	3.97E-02
165	IPI:IPI00012340.1	SFRS9	Splicing factor, arginine/serine-rich 9	2.17	3.76E-02
166	IPI:IPI00009634.1	SQRDL	Sulfide:quinone oxidoreductase, mitochondrial	2.30	3.34E-02
167	IPI:IPI00889196.2	UQCRFSL1	Cytochrome b-c1 complex subunit Rieske-like protein 1	2.44	3.28E-02
168	IPI:IPI00479145.2	KRT19	Keratin, type I cytoskeletal 19	2.52	1.23E-11
169	IPI:IPI00103027.4	LOC26010	Isoform 2 of SPATS2-like protein	2.80	9.51E-03
170	IPI:IPI00025512.2	HSPB1	Heat shock protein B1	3.02	2.23E-04

associated with good prognosis in patients with HCV infection [Harimoto et al., 2004].

The HSPs, which constitute a superfamily of chaperone proteins present in all cells and in all cell compartments [Hendrick and Hartl, 1993], are involved in a wide range of biological activities, including embryogenesis, morphogenesis, cell growth, differentiation, and apoptosis. Based on their molecular weights, HSPs have been divided into several subgroups: HSP90, HSP70, HSP60, and a family of small HSPs (sHSPs) [Mizrahi et al., 2010]. Ma et al. reported that overexpression of GRP78, one member of the HSP70 group, inhibited HBV replication via IFN-induced antiviral signaling pathways, which can be triggered by the innate immune system in response to viral infection [Ma et al., 2009]. However, whether HSPB1 can also affect hepatitis B virus replication remained unknown. To this end, we examined its effect on the HepG2.2.15 hepatoma cell line, which is transfected with 1-unit-length HBV DNA. To our surprise, we demonstrated that suppression of HSPB1 expression in HepG2.2.15 caused a nearly twofold increase of HBV production, as compared to the non-HBV expressing control cells. In addition, the levels of secreted HBsAg and HBeAg were also significantly increased. Furthermore, over-expression of HSPB1 in HepG2.2.15 led to a marked decrease in HBV production, suggesting that HSPB1 functions as an endogenous anti-HBV factor.

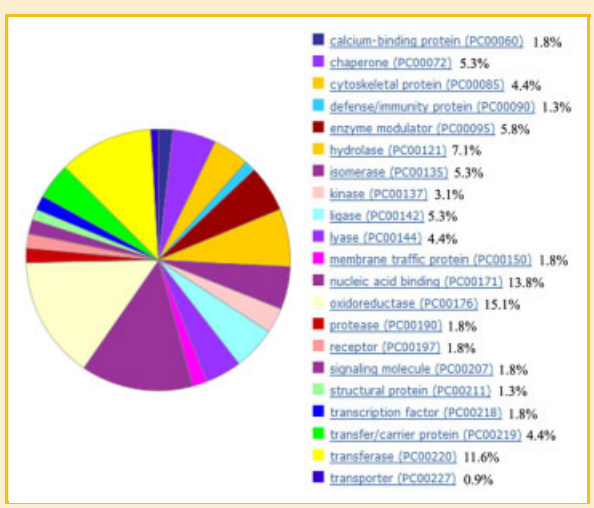

Fig. 2. Pie chart showing representation (%) of the various functional categories for the 170 differentially expressed proteins. Categories were identified based on the PANTHER classification system.

Subsequently, we focused on whether IFN-induced antiviral signaling pathways were activated by HSPB1 overexpression in HepG2.2.15 cells. As a result, increased mRNA levels of type I IFN and five downstream IFN-stimulated genes were observed, indicating an activation of these genes induced by HSPB1 transfection. However, three other effectors of the type I IFN-mediated antiviral signal, Mx1, OAS2, and OASL, showed minimal changes in the mRNA levels of related genes. Thus, our data demonstrates that HSPB1 functions as an anti-viral protein during HBV infection by specifically inducing type I IFN and some of the downstream antiviral effectors.

Up-regulation of DNAJB1 protein was also observed in HepG2.2.15. DNAJB1 belongs to the human Hsp40/DnaJ family that is involved in a diverse range of cellular functions, such as protein folding, translocation across membranes, and assembly and disassembly of multi-protein complex, and which acts by cooperating with Hsp70. Previous studies have shown that DNAJB1 interacts with the carboxyl-terminal region (aa 94-185) of the hepatitis B virus core protein and specifically accelerates degradation of the core and HBx proteins, ultimately suppressing HBV replication [Sohn et al., 2006b]. The authors also confirmed that HBx was the major target of DNAJB1 during the process of HBV replication inhibition, suggesting that DNAJB1 may represent an antiviral factor in infected cells [Sohn et al., 2006a]. In our study, we found that DNAJB1 was increased dramatically in HepG2.2.15, as

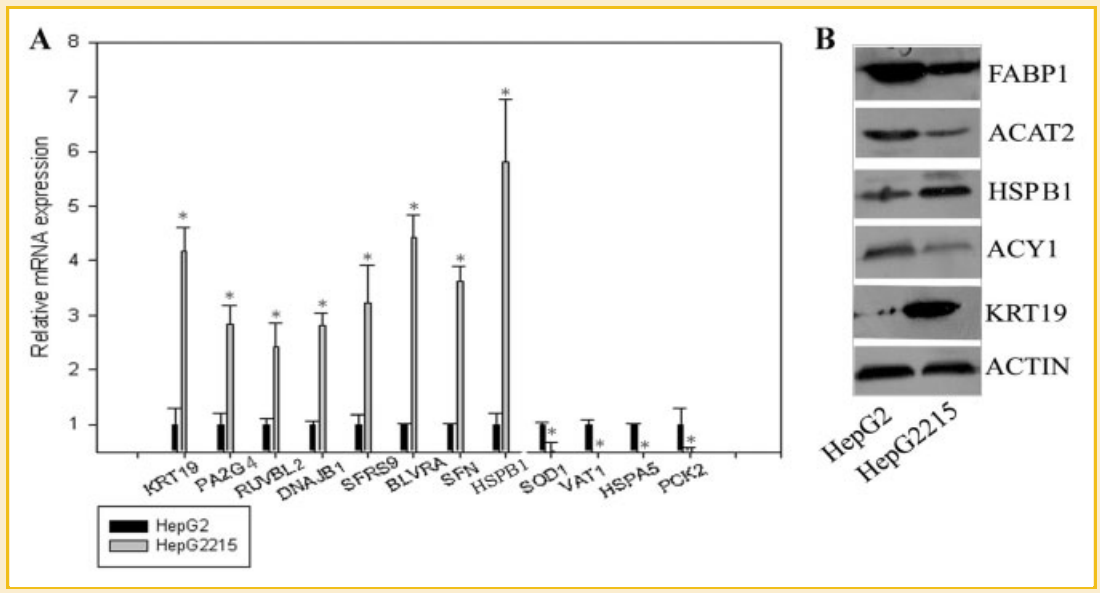

Fig. 3. Evaluation of the differentially expressed proteins in HepG2 and HepG2.2.15 cells. A: Real-time RT-PCR detected the relative mRNA expression levels of KRT19, PA2G4, RUVBL2, DNAJB1, SFRS9, BLVRA, SFN, HSPB1, SOD1, VAT1, HSPA5 and PCK2. 18S rRNA was used as the normalization standard. Bars indicate SD. $^{*}P \leq 0.05$ differ from control by *t*-test. B: A representative Western blot for HSPB1, KRT19, FABP1, ACAT2, and ACY1 expression in the two cell lines. $^{*}P < 0.05$ differ from control by *t*-test.

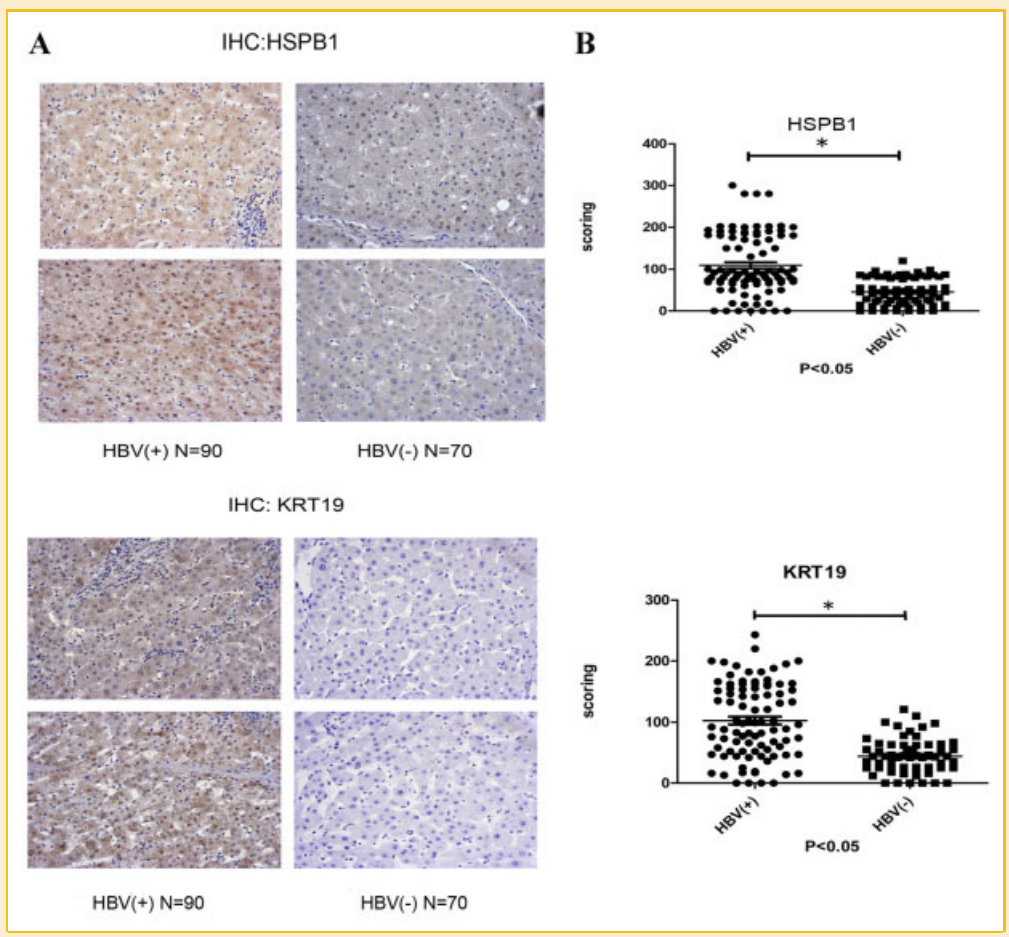

Fig. 4. Validation of HSPB1 and KRT19 overexpression using tissue microarrays. A: Representative images of the immunohistochemical detection of HSPB1 and KRT19 expression in HBV(+) tissues and HBV(−) tissues. B: IHC score values of HSPB1 and KRT19 are significantly higher in HBV(+) tissues than in HBV(−) tissues.

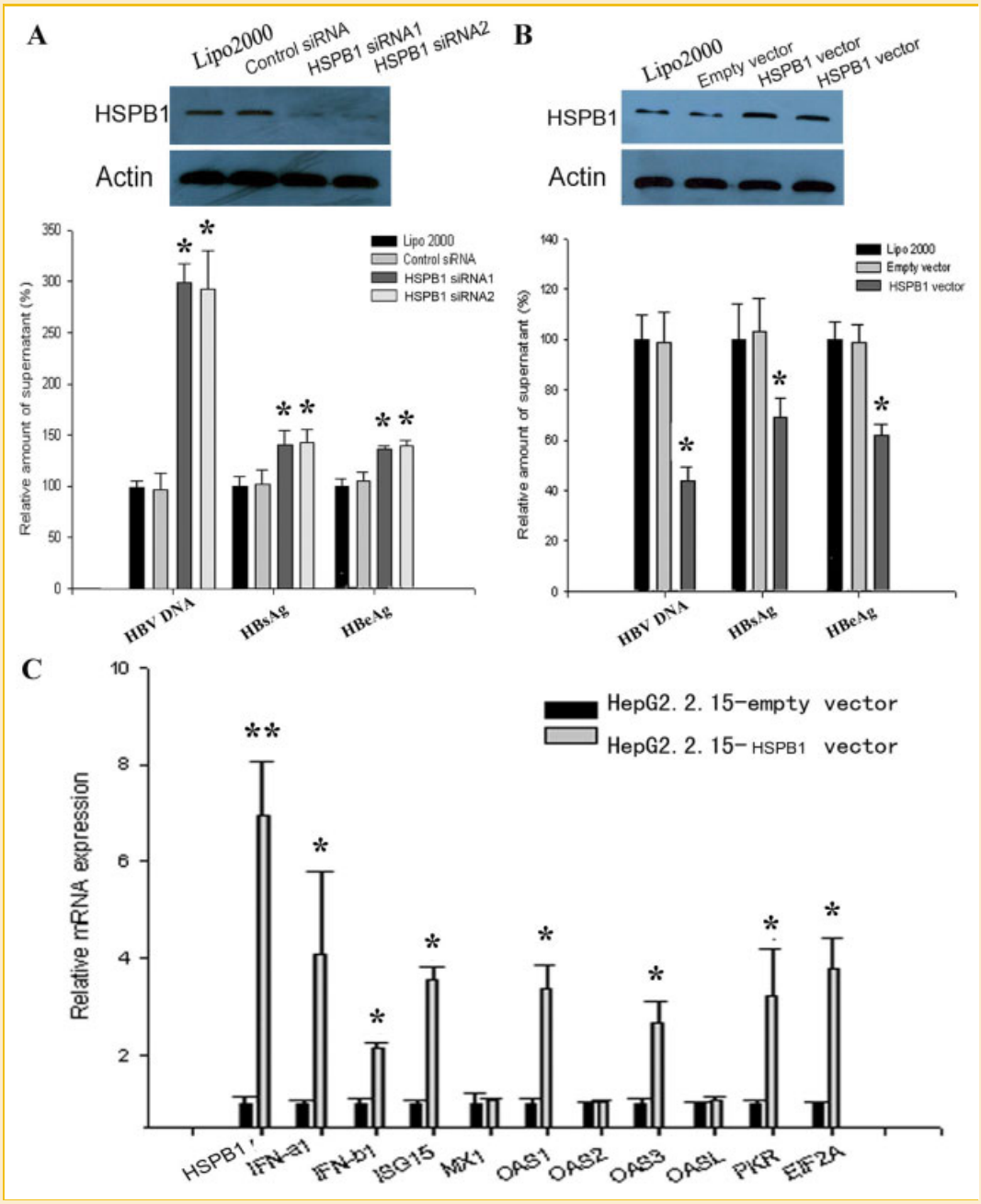

Fig. 5. Functional studies to assess the role of HSPB1 in HBV replication in HepG2.2.15 cells. A: Western blotting analysis showed that HSPB1-specific siRNAs significantly reduced HSPB1 protein levels in cell lysates. As compared to controls, silencing of HSPB1 expression by two different gene-specific siRNA sequences caused a nearly twofold increase of HBV production and significantly increased the secreted HBsAg and HBeAg levels. B: In contrast, HSPB1 overexpression led to a marked decrease in HBV production and secreted HBsAg and HBeAg levels. $^{*}P < 0.05$ differ from control by *t*-test. C: Real-time RT-PCR detected the relative mRNA expression levels of type I interferon and downstream interferon-stimulated genes after overexpresstion of HSPB1. The relative mRNA expression levels of type I IFN and five downstream IFN-stimulated genes were elevated, while no obvious changes were detected for the other three IFN-stimulated genes. $^{*}P < 0.05$, $^{**}P < 0.01$.

compared to levels detected in HepG2. It is very likely that DNAJB1 was induced by HBV infection and exerts inhibitory functions on virus replication.

Interestingly, another protein found in our study that was remarkably up-regulated in HepG2.2.15 is another heat shock protein, HSPA8. Early in 1997, it was reported that HSPA8 participates in HBV morphogenesis through interaction with the envelope protein [Loffler-Mary et al., 1997]. Moreover, Wang et al. [2010] demonstrated that introducing HSPA8 into HepG2.2.15 cells increased HBV replication, while knockdown of HSPA8 expression by RNA interference largely inhibited HBV replication with no cytotoxicity to the host cells. Moreover, the anti-HBV effect of oxymatrine was shown to be mediated by destabilizing HSPA8 mRNA, implicating HSPA8 as an anti-HBV drug target [Wang et al.,

2011]. Collectively, these data have revealed that HSPA8 may play an important role in assisting HBV replication.

Complement component 3 (C3), which plays a central role in activation of the complement system and contributes to innate immunity, was found to be suppressed by HBV infection in HepG2.2.15 cells, as compared to that in HepG2. In fact, decreased expression levels of C3 have been reported previously in serum from both acute viral hepatitis B and HBV-related chronic liver patients [Joshi et al., 1990]. The decreased C3 levels may be attributed to decreased synthesis and increased consumption by the enhanced levels of circulating immune complex. As host innate immunity is inhibited to some extent during HBV infection, there must be another immune cellular mechanism accounting for the decrease of C3 level.

Finally, our study identified several other proteins, including MVP, PA2G4, NPM1, DDX21, and ACAT2, which had not been previously associated with HBV replication, but which have been implicated in other viral infections, such as HCV [Liu et al., 2012], influenza [Bortz et al., 2011], HIV [Naji et al., 2012], and norovirus [Chang, 2009]. A recent study found that during HCV infection MVP induced cellular antiviral responses and characterized the protein as a novel virus-induced host factor that functioned through up-regulation of type I IFN production [Liu et al., 2012]. These features are similar to our findings for HSPB1. The correlation between each of the differentially expressed proteins and HBV replication in HepG2.2.15 will be a focus of our future study.

Sustained inhibition of virus replication is one of the major challenges facing HBV treatment. The fact that the underlying mechanism of HBV replication remains unclear has been a significant impediment to resolving the issue. In this study, we focused our attention on those proteins with altered expression levels in the HepG2.2.15 cell line. As a result, 170 differentially expressed proteins possibly associated with HBV replication were identified, and the correlation of HSPB1 with HBV replication was confirmed. We demonstrated, for the first time, that HSPB1 may function as an anti-viral protein during HBV infection by specifically inducing type I interferon and some of its downstream antiviral effectors. The precise role of each of these proteins in the HBV replication should be investigated in future studies. We believe that HSPB1 may represent a novel therapeutic target for pharmacologic intervention of HBV replication.

ACKNOWLEDGMENTS

This work was supported by program for Changjiang Scholars and Innovative Research Team in University (no. IRT0872), National Natural Science Foundation of China (no. 30801348, and 30900507), National Science and Technology Major Project of China (no. 2008ZX10002-006), and China Postdoctoral Science Foundation Founded Project (no. 20070410210).

REFERENCES

Bortz E, Westera L, Maamary J, Steel J, Albrecht RA, Manicassamy B, Chase G, Martinez-Sobrido L, Schwemmle M, Garcia-Sastre A. 2011. Host- and strain-specific regulation of influenza virus polymerase activity by interacting cellular proteins. MBio 2:e00151-11.

Chang KO. 2009. Role of cholesterol pathways in norovirus replication. J Virol 83:8587–8595.

Ciocca DR, Jorge AD, Jorge O, Milutin C, Hosokawa R, Diaz Lestren M, Muzzio E, Schulkin S, Schirbu R. 1991. Estrogen receptors, progesterone receptors and heat-shock 27-kD protein in liver biopsy specimens from patients with hepatitis B virus infection. Hepatology 13:838–844.

Feng JT, Liu YK, Song HY, Dai Z, Qin LX, Almofti MR, Fang CY, Lu HJ, Yang PY, Tang ZY. 2005. Heat-shock protein 27: A potential biomarker for hepatocellular carcinoma identified by serum proteome analysis. Proteomics 5:4581–4588.

Gorg A, Obermaier C, Boguth G, Harder A, Scheibe B, Wildgruber R, Weiss W. 2000. The current state of two-dimensional electrophoresis with immobilized pH gradients. Electrophoresis 21:1037–1053.

Gorg A, Weiss W, Dunn MJ. 2004. Current two-dimensional electrophoresis technology for proteomics. Proteomics 4:3665–3685.

Gygi SP, Rist B, Gerber SA, Turecek F, Gelb MH, Aebersold R. 1999. Quantitative analysis of complex protein mixtures using isotope-coded affinity tags. Nat Biotechnol 17:994–999.

Harimoto N, Shimada M, Aishima S, Kitagawa D, Itoh S, Tsujita E, Maehara S, Taketomi A, Tanaka S, Shirabe K, Maehara Y. 2004. The role of heat shock protein 27 expression in hepatocellular carcinoma in Japan: Special reference to the difference between hepatitis B and C. Liver Int 24:316–321.

Hendrick JP, Hartl FU. 1993. Molecular chaperone functions of heat-shock proteins. Annu Rev Biochem 62:349–384.

Joshi N, Ayesha Q, Habibullah CM. 1990. Immunological studies in HBV-related chronic liver diseases. Indian J Pathol Microbiol 33:351–354.

Lai CL, Ratziu V, Yuen MF, Poynard T. 2003. Viral hepatitis B. Lancet 362:2089–2094.

Lee TH, Tai DI, Cheng CJ, Sun CS, Lin CY, Sheu MJ, Lee WP, Peng CY, Wang AH, Tsai SL. 2006. Enhanced nuclear factor-kappa B-associated Wnt-1 expression in hepatitis B- and C-related hepatocarcinogenesis: Identification by functional proteomics. J Biomed Sci 13:27–39.

Lim SO, Park SG, Yoo JH, Park YM, Kim HJ, Jang KT, Cho JW, Yoo BC, Jung GH, Park CK. 2005. Expression of heat shock proteins (HSP27, HSP60, HSP70, HSP90, GRP78, GRP94) in hepatitis B virus-related hepatocellular carcinomas and dysplastic nodules. World J Gastroenterol 11:2072–2079.

Liu S, Hao Q, Peng N, Yue X, Wang Y, Chen Y, Wu J, Zhu Y. 2012. Major vault protein: A virus-induced host factor against viral replication through the induction of type-I interferon. Hepatology 56:57–66.

Livak KJ, Schmittgen TD. 2001. Analysis of relative gene expression data using real-time quantitative PCR and the 2(-Delta Delta C(T)) Method. Methods 25:402–408.

Loffler-Mary H, Werr M, Prange R. 1997. Sequence-specific repression of cotranslational translocation of the hepatitis B virus envelope proteins coincides with binding of heat shock protein Hsc70. Virology 235:144–152.

Lu JW, Hsia Y, Yang WY, Lin YI, Li CC, Tsai TF, Chang KW, Shieh GS, Tsai SF, Wang HD, Yuh CH. 2012. Identification of the common regulators for hepatocellular carcinoma induced by hepatitis B virus X antigen in a mouse model. Carcinogenesis 33:209–219.

Ma Y, Yu J, Chan HL, Chen YC, Wang H, Chen Y, Chan CY, Go MY, Tsai SN, Ngai SM, To KF, Tong JH, He QY, Sung JJ, Kung HF, Cheng CH, He ML. 2009. Glucose-regulated protein 78 is an intracellular antiviral factor against hepatitis B virus. Mol Cell Proteomics 8:2582–2594.

Mirgorodskaya OA, Kozmin YP, Titov MI, Korner R, Sonksen CP, Roepstorff P. 2000. Quantitation of peptides and proteins by matrix-assisted laser desorption/ionization mass spectrometry using (18)O-labeled internal standards. Rapid Commun Mass Spectrom 14:1226–1232.

Mizrahi T, Heller J, Goldenberg S, Arad Z. 2010. Heat shock proteins and resistance to desiccation in congeneric land snails. Cell Stress Chaperones 15:351–363.

Naji S, Ambrus G, Cimermancic P, Reyes JR, Johnson JR, Filbrandt R, Huber MD, Vesely P, Krogan NJ, Yates JR 3rd, Saphire AC, Gerace L. 2012. Host cell interactome of HIV-1 rev includes RNA helicases involved in multiple facets of virus production. Mol Cell Proteomics 11: M111 015313.

Ross PL, Huang YN, Marchese JN, Williamson B, Parker K, Hattan S, Khainovski N, Pillai S, Dey S, Daniels S, Purkayastha S, Juhasz P, Martin S, Bartlet-Jones M, He F, Jacobson A, Pappin DJ. 2004. Multiplexed protein quantitation in *Saccharomyces cerevisiae* using amine-reactive isobaric tagging reagents. Mol Cell Proteomics 3:1154–1169.

Sohn SY, Kim JH, Baek KW, Ryu WS, Ahn BY. 2006a. Turnover of hepatitis B virus X protein is facilitated by Hdj1, a human Hsp40/DnaJ protein. Biochem Biophys Res Commun 347:764–768.

Sohn SY, Kim SB, Kim J, Ahn BY. 2006b. Negative regulation of hepatitis B virus replication by cellular Hsp40/DnaJ proteins through destabilization of viral core and X proteins. J Gen Virol 87:1883–1891.

Wang YP, Liu F, He HW, Han YX, Peng ZG, Li BW, You XF, Song DQ, Li ZR, Yu LY, Cen S, Hong B, Sun CH, Zhao LX, Kreiswirth B, Perlin D, Shao RG, Jiang JD. 2010. Heat stress cognate 70 host protein as a potential drug target against drug resistance in hepatitis B virus. Antimicrob Agents Chemother 54:2070–2077.

Wang YP, Zhao W, Xue R, Zhou ZX, Liu F, Han YX, Ren G, Peng ZG, Cen S, Chen HS, Li YH, Jiang JD. 2011. Oxymatrine inhibits hepatitis B infection with an advantage of overcoming drug-resistance. Antiviral Res 89:227–231.

Wright TL. 2006. Introduction to chronic hepatitis B infection. Am J Gastroenterol 101(Suppl. 1):S1–S6.